Journal for Research in Applied Sciences and Biotechnology

www.jrasb.com

ISSN: 2583-4053

Volume-3 Issue-1 || February 2024 || PP. 99-108

https://doi.org/10.55544/jrasb.3.1.17

The Impact of Argon Flow Rates on Plasma Behavior in Plasma Jet Systems for Medical Applications

Alaa Raad[1] and Hanaa Essa[2]

[1]Department of Physics, College of Science, University of Tikrit, Tikrit, IRAQ.

[2]Department of Physics, College of Science, University of Tikrit, Tikrit, IRAQ.

[1]Corresponding Author: alaaraad319@gmail.com

www.jrasb.com || Vol. 3 No. 1 (2024): February Issue

Received: 30-01-2024	**Revised:** 01-01-2024	**Accepted:** 02-02-2024

ABSTRACT

This research presents a thorough spectroscopic investigation of atmospheric- plasma generated by a plasma jet. The study examines the plasma behavior under varying flow rates of argon gas. A primary objective is to identify the optimal flow rate that facilitates the application of the generated plasma in sterilization and bacterial eradication operations. The findings establish a correlation between argon flow and critical plasma parameters, specifically noting variations in electron temperature (T_e) & electron number density (n_e). Crucially, the study demonstrates that lower argon flow rates are more effective in generating active species such as hydroxyl and NO reactive species. The results of this investigation hold significant promise for advancing our comprehension of plasma jet technology's utility in sterilization or medical treatment processes, emphasizing the importance of gas flow optimization for these applications.

***Keywords*-** Plasma jet, Plasma parameters, Optical Emission Spectroscopy.

I. INTRODUCTION

The exploration of plasma characteristics through spectroscopic analysis has become a pivotal focus within the realm of different scientific fields [1]. In this context, various types of plasmas are utilized, promising and straightforward techniques, for advancing our comprehension of intricate physical processes [2].

Different types of plasmas have been harnessed for numerous applications, showing their versatility in various scientific and technological domains [3]. One particularly notable and widely employed technique is plasma jet technique, which, due to its simplicity, holds significant promise for enhancing our understanding of complex physical processes [4]. Plasma jet technology is not only confined to laboratory settings but has also found practical applications in medical contexts, particularly in the field of sterilization [5]. The unique properties of plasma, including its ability to generate reactive species, make it an effective tool for inhibiting bacteria and ensuring sterilization. This dual application underscores the multifaceted nature of plasma jet technology, illustrating its potential impact on both scientific research and practical, real-world applications. Plasma jet technology has found applications in medical fields and sterilization processes, marking it as a useful tool with multifaceted implications [6].

The spectroscopic analysis serves as a powerful tool offering a nuanced perspective into the behavior and composition of plasma, providing invaluable insights into the interactions among its constituent species [7]. This approach enables researchers to unravel the intricacies of interactions between atoms and ions, yielding crucial information regarding their energies, densities, and elemental compositions [8]. Optical emission spectroscopy (OES) stands out among the array of spectroscopic methods frequently employed to analyze plasma characteristics [9]. In OES, electromagnetic radiation emitted by excited atoms and ions in the plasma is detected and analyzed. This emission results from

ISSN: 2583-4053
Volume-3 Issue-1 || February 2024 || PP. 99-108
https://doi.org/10.55544/jrasb.3.1.17

transitions between energy levels of these species, delivering valuable information about their populations, energy distributions, and temperatures. OES proves instrumental in identifying ratios of ions and neutrals present in the plasma, thereby offering insights into the composition and ionization state of the plasma species [10]. [11]. The application of spectroscopic study allows scientists to discern variations in plasma behavior, prompting investigations into elemental distribution, species concentration, and energy distributions [12]. This comprehensive examination advance our understanding of plasma dynamics, thereby contributing to the optimization of plasma-based technologies in various scientific and industrial domains [13].

The primary objective of this investigation is to analyze the influence of Ar flow rates within a plasma jet system on the diverse behaviors exhibited by the plasma. This study aims to gain a comprehensive understanding of various plasma characteristics, encompassing electron density, ion density, electron temperature, and species composition. The assessment of these attributes will be conducted through the utilization of optical emission spectroscopy (OES). Subsequently, the study aims to pinpoint the optimal flow rate that effectively enables the application of the generated plasma in operations related to sterilization and medical treatment.

II. EXPERIMENTAL SETUP

The experimental configuration, as depicted in Figure 1, comprises a plasma jet system featuring a tube housing externally electric electrodes. The tube facilitates the flow of gas, which undergoes ionization upon exposure to the electric current generated between the electrodes. In this setup, plasma is ignited within the nozzle/tube and subsequently directed outside the target area for treatment via gas flow. The plasma jet employs argon gas. A high-voltage power source produces a pulsed waveform with a voltage of 7kV and a frequency of 25kHz. Plasma generation involves subjecting the gas to a voltage.

A spectrometer (Thorlabs- CCS 100/M) was utilized to diagnosed the emissions from the plasma over a wavelength range spanning from 200 to 900 nm. Importantly, these analyses were performed under varying Ar flow rates.

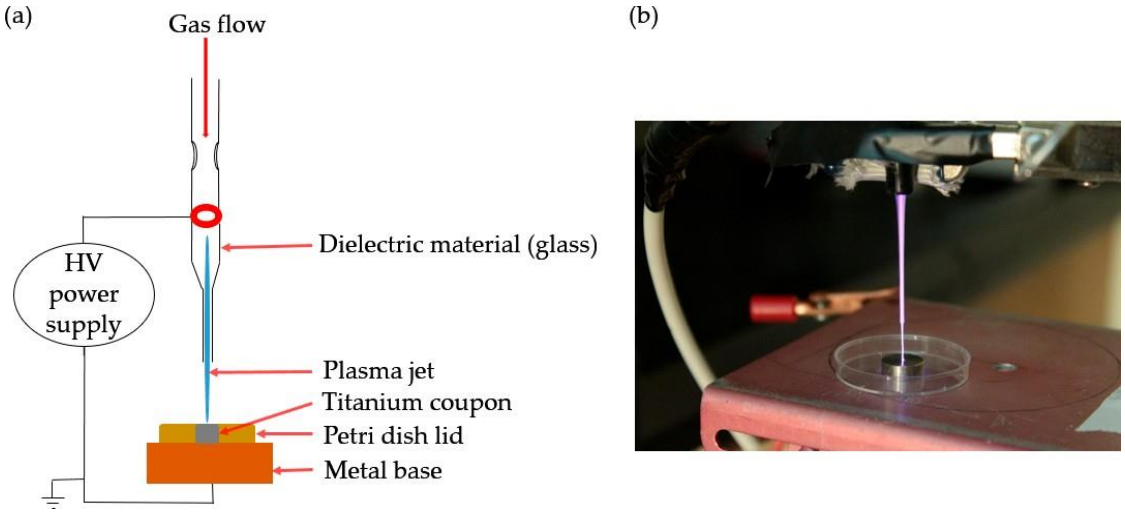

Figure 1: A schematic and photograph for plasma jet configuration

III. RESULTS AND DISCUSSIONS

Figure 2 shows the spectra emitted from the plasma generated from atmospheric plasma jet technology using Ar gas at different gas flow rates (2, 4, 6, 8, 12, and 16 l/min). The emitted lines are combined with the atomic standard lines for argon (Ar I) from the National Institute of Standards and Technology data (NIST) [14], as well as the molecular spectral lines for nitrogen [15]. The spectrum appears to be composed of two distinct regions, one of which is within the wavelength range from approximately 700 to 900 nm, which belongs to the atomic argon spectrum, and the other lies within the wavelength range from approximately 300 to 450 nm, which belongs to the molecular spectrum of nitrogen, which is the largest component of atmospheric air. The intensity of the Ar spectral lines within a single sample varies in intensity due to the difference in the transition probability, and also based on the principle of the Boltzmann distribution according to the plasma temperature [16], in addition to the content of the species within the plasma. The absence of ionic spectral lines indicates the low content of Ar ions due to the low degree of ionization.

In general, the intensity of the emission line increases with the increase of the argon gas flow to a certain extent due to the increase in its content inside the

ISSN: 2583-4053

Volume-3 Issue-1 || February 2024 || PP. 99-108

https://doi.org/10.55544/jrasb.3.1.17

plasma, which leads to an increase in the possibility of irritating collision of the plasma electrons with the argon atoms that excite them, and then the process of emitting photons when the electrons return to a lower energy level. It can also be noted that the intensity of the spectral lines increases at different rates for different lines depending on the plasma temperature, based on the Boltzmann distribution [17]. While the large increase in flow led to a decrease in intensity due to the increase in elastic collisions, which cause the transfer of part of the energy of the electrons to the atoms, which prevents the energy of the electrons from reaching sufficient energy to excite the atoms before they collide again. There are some strange low-intensity peaks that may be due to atmospheric components [15].

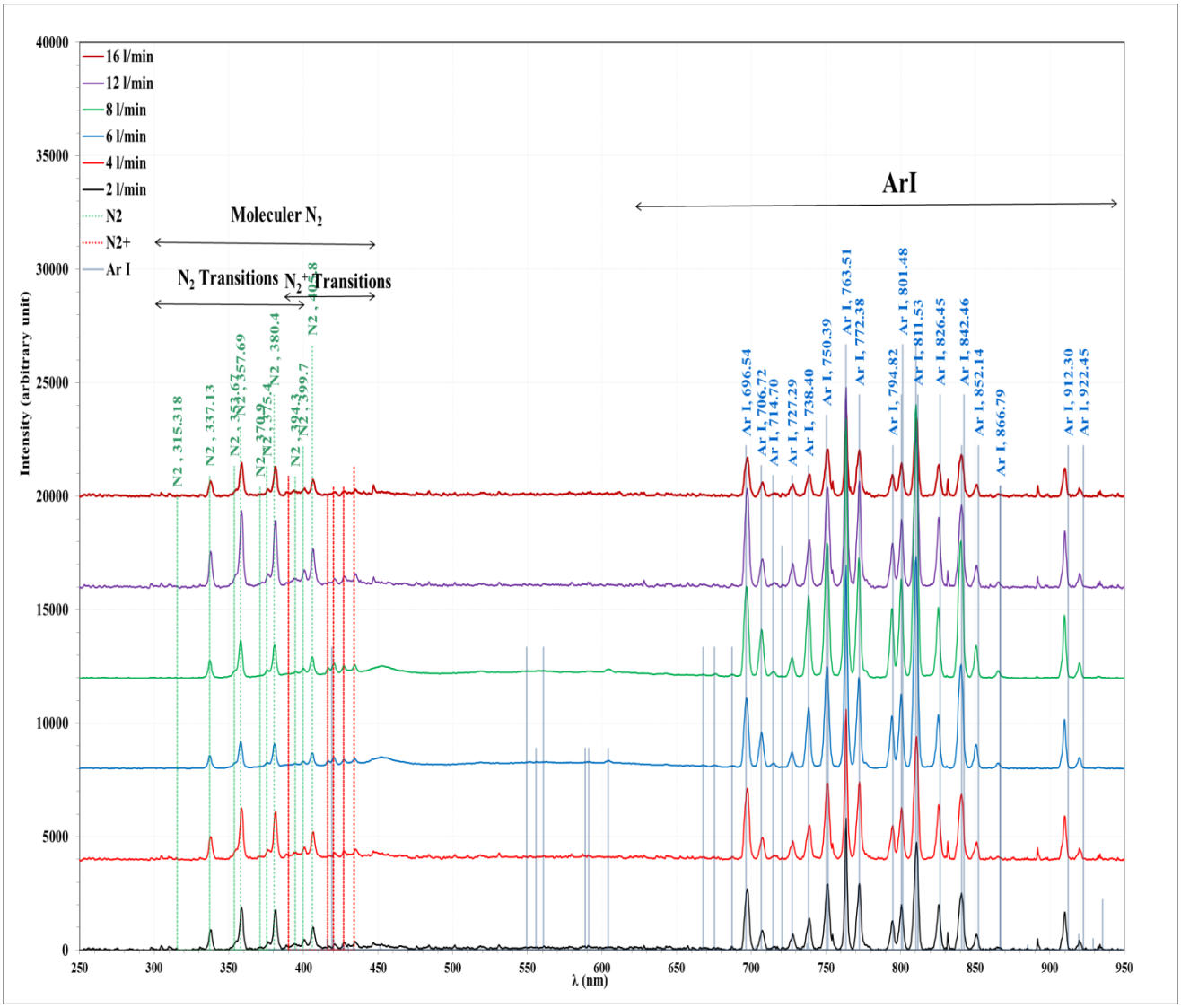

Figure 2: Spectra of plasma emitted by plasma jet technology using different flow rates of Ar.

Figure 3 shows the change in intensity of the spectral lines emitted by plasma jet technology with the flow rate of Ar for the spectral line (375 nm) for nitrogen molecule (N_2) induced from atmosphere, and the spectral line (763.5 nm) for Ar, and the ratio between the intensities of the two lines. We note that the highest intensity of the spectral line for nitrogen was at a flow of (12 l/min), while the highest intensity of the Ar line was at a flow of Ar (8 l/min). The reason for the difference in the location of the intensity peak of the two gases is due to the difference in the energy rate of the electrons inside the plasma, with a difference in the energy required for the irritating collision of both gases. We notice a change in the intensity ratio Between the two lines, it will be the greatest possible at a flow of (6 l/min).This change in ratio is the reason for the color of the plasma generated by the plasma jet system varying between violet and red depending on the flow speed [18].

Journal for Research in Applied Sciences and Biotechnology

ISSN: 2583-4053

Volume-3 Issue-1 || February 2024 || PP. 99-108

www.jrasb.com

https://doi.org/10.55544/jrasb.3.1.17

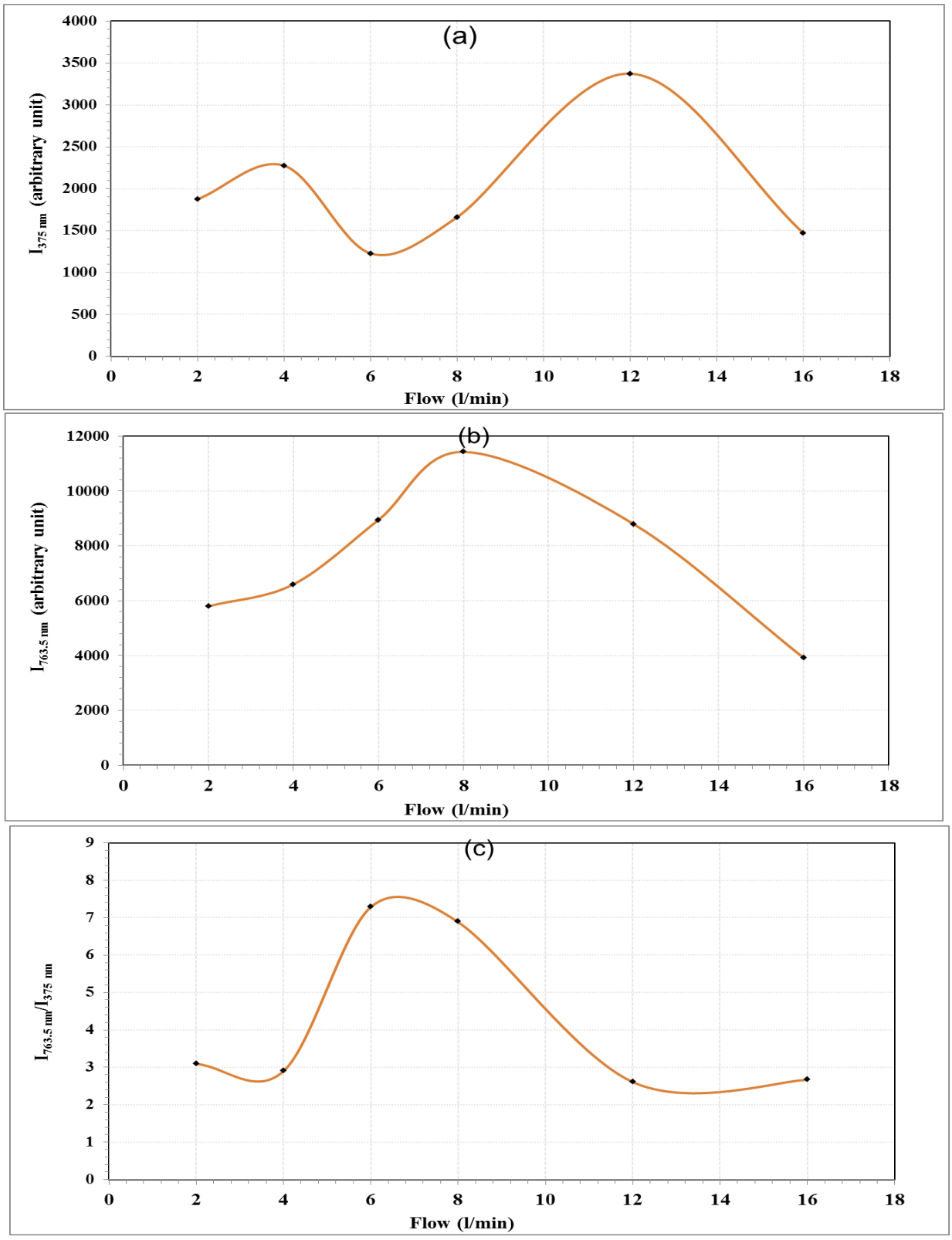

Figure 3: Change in the intensity of the spectral lines emitted by plasma jet technology with the flow rate of Ar (a) The intensity of the 375 nm spectral line for nitrogen, (b) The intensity of the 763.5 nm for Ar spectral line , and (c) The relative ratio between the two lines

Figure 4 shows matching the Lorentz distribution of the spectral line (763.5 nm) of Ar to

Journal for Research in Applied Sciences and Biotechnology

www.jrasb.com

ISSN: 2583-4053

Volume-3 Issue-1 || February 2024 || PP. 99-108

https://doi.org/10.55544/jrasb.3.1.17

calculate the Stark broadening of the spectral line emitted by plasma jet technology at different Ar flow rates. The full line width (Δλ) is found using the standard Lorentzian curve, which is used to calculate the electron density for each flow state. The calculation is based on the electron impact factor (ω_m), which is equal to (0.0074 nm) at an electron density of 1×10^{16} cm^{-3} for this spectral line [19]. It can be observed that the line width varies with the flow rates of argon gas.

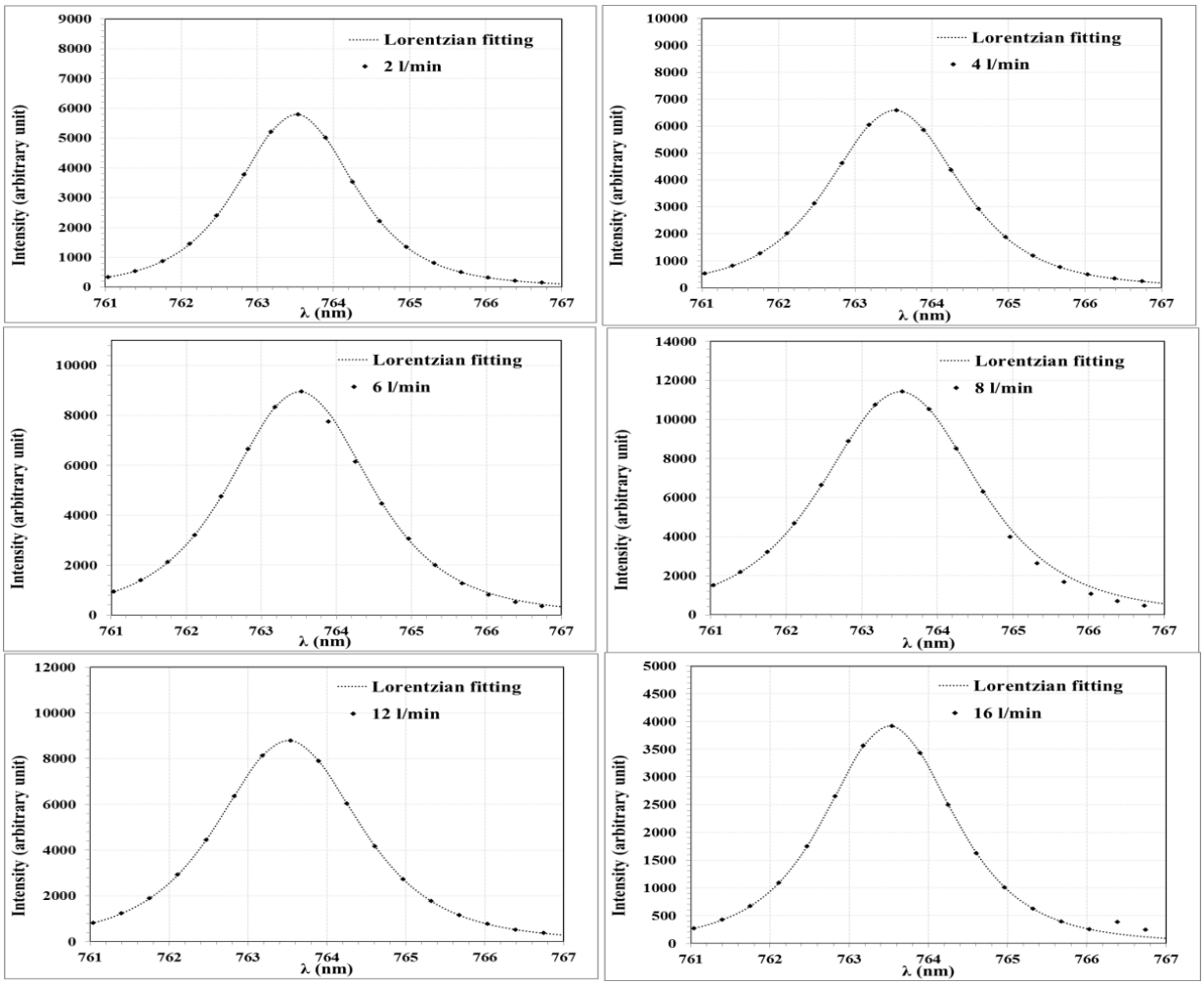

Figure 4: Matching with the broadening with Lorentz curve for the Ar 763.5 nm to calculate electron number density using Stark broadening for plasma jet at different Ar flow rates.

Electron temperature (T_e) values were determined by a Boltzmann plot using the intensities of five spectral lines of the Ar atom shown in Table 1 according to NIST data [17].

Table 1: NIST Ar-I emission lines that were used in the electron temperature calculations.

λ (nm)	$A_{ji}.g_j\times10^7$	Energy lower level (eV)	Energy of upper level (eV)
696.5431	1.920	11.54835	13.327857
706.7218	1.900	11.54835	13.302227
727.2936	0.549	11.62359	13.327857
738.3980	4.240	11.62359	13.302227
750.3869	4.450	11.82807	13.479887

These lines were used to determine the plasma temperature of the plasma under different conditions in all spectra in this study as shown in Figure 5. The electron temperature (T_e) was calculated using the relationship between $\boldsymbol{ln}\left(\frac{I_{ji}\lambda_{ji}}{hcg_jA_{ji}}\right)$ versus the upper energy level (E_j). The figure displays the best-fitting linear relationship equations within the shapes. The values of T_e are equal to the inverse of the slope of the given lines. The R^2 values

ISSN: 2583-4053
Volume-3 Issue-1 || February 2024 || PP. 99-108
https://doi.org/10.55544/jrasb.3.1.17

presented in each figure indicate values higher than 0.9 which indicate good linear fit with practical values.

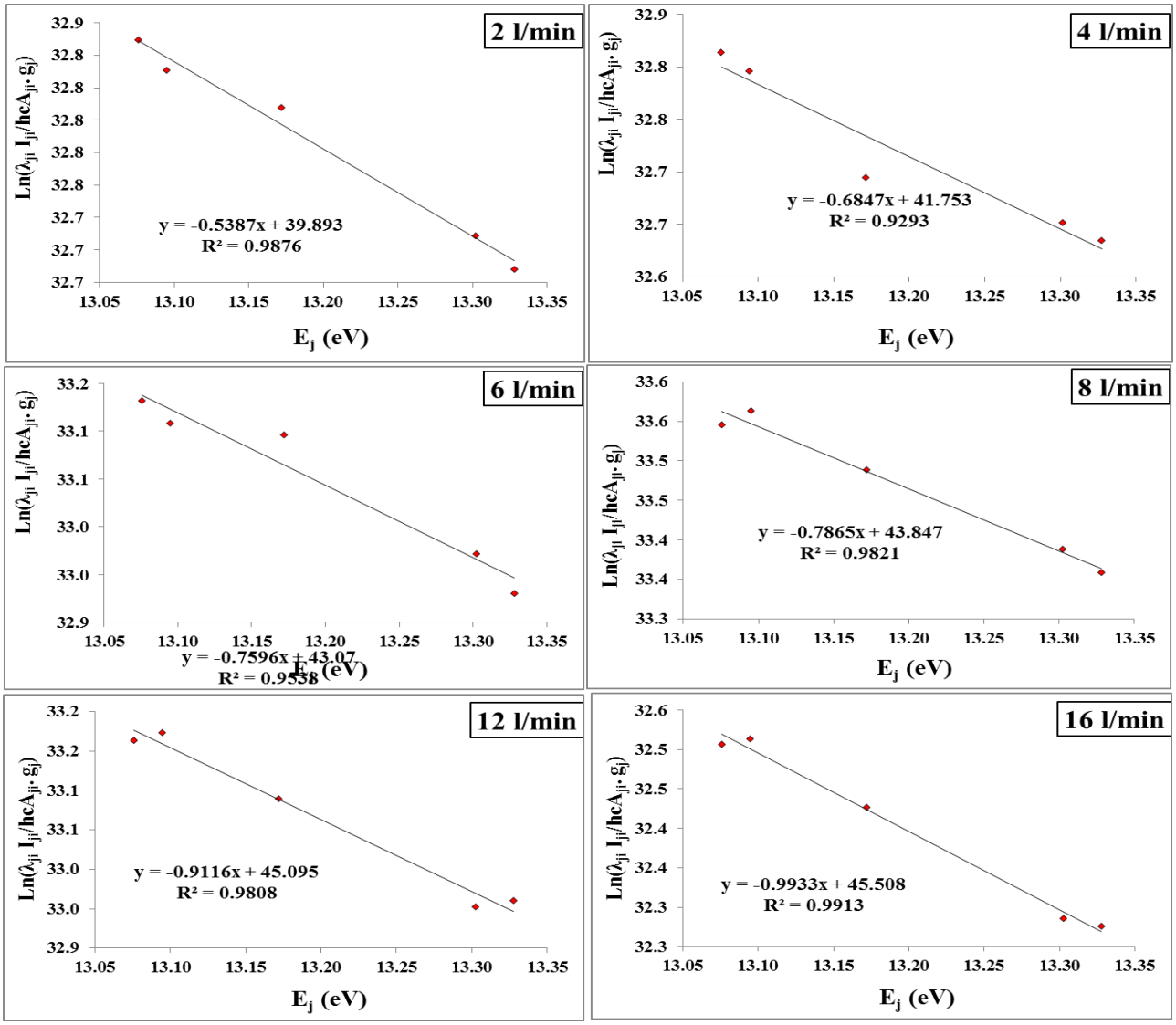

Figure 5: Boltzmann-plot using Ar atomic spectral lines emitted by plasma jet technology at different Ar flow rates to calculate the plasma temperature.

Figure 6 shows the variation of electron temperature (T_e) and electron number density (n_e) of plasma generated by plasma-jet technique with the flow rate of Ar. Increasing the Ar flux from (2 l/min) to (8 l/min) led to an increase in n_e due to the increased probability of ionizing collisions, which leads to the generation of additional electrons that perpetuate the existence of the plasma [20]. A further increase in the flow rate leads to an opposite behavior with a decrease in n_e due to a decrease in the energy rate of the electrons, as a result of increase in the number of collisions that suppress the electrons energy and prevent them from reaching sufficient energies to ionize the atoms due to the decrease in the cross-section of ionizing collisions with the decrease in the energy of the electrons [21]. On the other hand, we notice a steady decrease in the electron temperature (T_e) with the increase of the Ar flow due to the increase in non-ionizing collisions between electrons and other particles [22].

Journal for Research in Applied Sciences and Biotechnology
www.jrasb.com

ISSN: 2583-4053
Volume-3 Issue-1 || February 2024 || PP. 99-108
https://doi.org/10.55544/jrasb.3.1.17

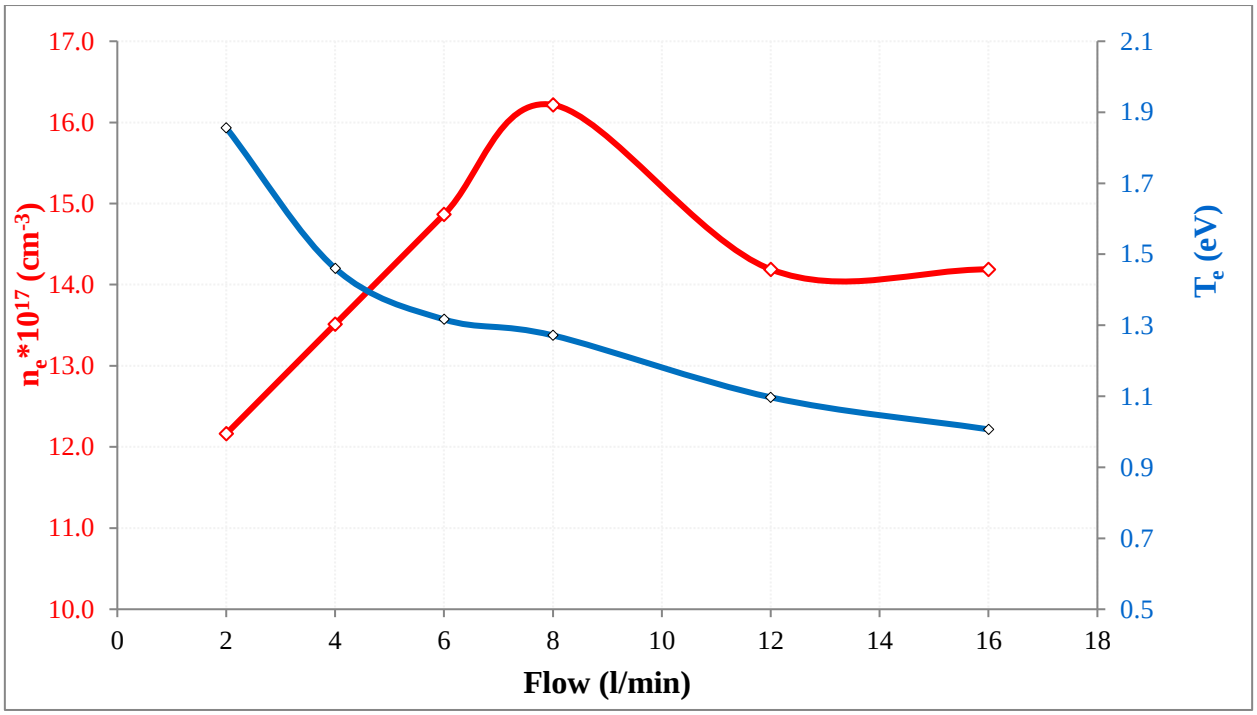

Figure 6: variation of plasma temperature and number density of electrons with the Ar flow rate.

Other plasma parameters were determined, including Debye length (λ_D), Debye number (N_D), and plasma frequency (f_p). Table 2 shows the plasma parameters at different Ar flows. All plasma parameters satisfy the plasma criteria. Changes in the temperature and number density of the plasma lead to a significant change in other plasma parameters. The plasma frequency increases to reach its peak at 8 l/min flow due to the dependence of the plasma frequency on its density. This frequency determines the frequencies of electromagnetic waves that interact with the plasma. While the Debye length decreases with increasing flow, as the increase in the number density of electrons and the decrease in plasma temperature lead to an increase in the response of the plasma to external fields, so the penetration depth of the electric fields decreases.

Table 2: Parameters of plasma emitted by plasma jet using different argon flow rates

Flow (l/min)	Te (eV)	Δλ (nm)	$n_{e*}10^{17}$ (cm^{-3})	f_p (Hz) *10^{12}	λ_D *10^{-6}(cm)	N_D
2	1.856	1.800	12.162	9.903	9.179	3940
4	1.460	2.000	13.514	10.439	7.724	2609
6	1.316	2.200	14.865	10.949	6.992	2129
8	1.271	2.400	16.216	11.435	6.579	1934
12	1.097	2.100	14.189	10.697	6.533	1657
16	1.007	2.100	14.189	10.697	6.259	1457

Figure 7 shows the molecular spectrum of nitrogen emitted from plasma jet technique using a 12 l/min flow rate of Ar as an example to illustrate the type of emissions in the spectrum. The electron atoms in the ground state fill the two metastable levels at energies 11.5 eV and 11.72 eV. When the excited argon (Ar*) mixed with neutral molecular nitrogen N_2 in its vibrational ground state $X^1\Sigma_g$ excited to one of the vibrational levels of the $C^3\Pi_u$ state because the energy of the Ar* states matches the necessary excitation energy of 11.1 eV. The discharge region also contains other types of molecular nitrogen, such as positive ions of the nitrogen molecule (N_2^+) resulting from direct ionization of neutral molecules. Depending on the energy of the incident electron, the ions may be pushed either to their vibrational ground state $X^2\Sigma_g$ or directly to a higher vibrational state. The excited states then decay spontaneously, giving rise to an emission spectrum with intensity proportional to the pumping amount of the upper bands.

Therefore, the spectrum shows two types of emissions located in two overlapping spectral regions, the first of which is due to the nitrogen molecule (N2) from 320 nm to 410 nm and the second to the nitrogen ion (N_2^+) from 390 nm to 440 nm. The peak located at 337.13 nm

ISSN: 2583-4053

Volume-3 Issue-1 || February 2024 || PP. 99-108

https://doi.org/10.55544/jrasb.3.1.17

represents the emission from the energy difference of the electronic transition between two states with the same vibrational energy (Δv=0). In addition to other groups located to the right and left of this peak of the spectrum resulting from a transition between two electronic levels for two different vibrational states. Each group consists of several peaks because the energy difference between each two successive vibrational levels is not equal. Therefore, the transition, for example, between two vibrational states 2-1 differs in energy from the transition 3-2, even though Δv=-1 in both cases.

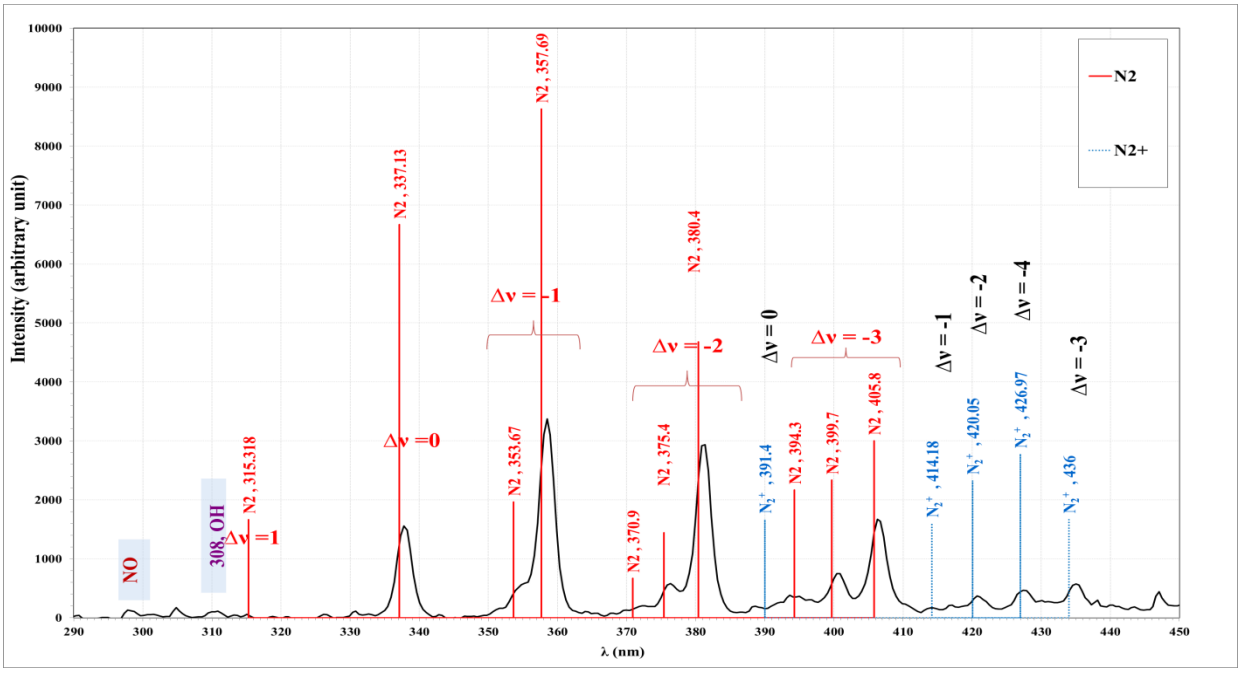

Figure 7: Molecular spectrum of nitrogen emitted from plasma jet in atmosphere using 12 l/min Ar flow rate

The spectrum also shows two small peaks located at 310 nm and 298 nm, which belong to the hydroxyl radical (OH) and nitrogen oxide (NO). These free radicals, such as OH and NO, play an important role in killing bacteria and sterilization processes. The hydroxyl radical (OH) has strong oxidizing properties. Its ability to interact with bacteria depends on its concentration and presence in the medium. Hydroxyl radical can lead to oxidation and destruction of bacterial cell membranes, contributing to their killing. Nitrogen oxide, which is formed during electrical discharge in the atmosphere, also has antibacterial properties. Nitrogen oxide can react with organic compounds in bacteria, inhibiting the activity of vital enzymes and thus killing the bacteria. Application of these free radicals in sterilization operations against bacteria and viruses by producing them using electrical discharge systems, which destroy microorganisms and improve environmental cleanliness.

Figure 8 shows the spectra emitted from the plasma generated using the atmospheric plasma jet technique using argon gas at different flow rates in the region from 290 nm to 450 nm. The intensity of the spectral lines varies within a single nitrogen sample due to the difference in the transfer potential, and also based on the vibrational temperature of the molecule, which plays an important role in the properties of the plasma formed. The spectral lines of the neutral hydrogen molecule appeared higher than those of the hydrogen ion, N_2^+, which indicates a low degree of ionization, which is a general characteristic of cold plasma.

In general, the intensity of the emission line increases with increasing Ar gas flow, reaching its peak at a gas flow of 12 l/min, then decreasing at 14 l/min. It can also be noted that the intensity of the spectral lines increases at different rates for different lines depending on the temperature. It can be noted that the intensity of the lines belonging to active species such as OH and NO are greatest at low and large gas flows, while they almost disappear at average flow values of 6 and 8 l/min. The reason for the lower content of active species in these flows may be due to the higher degree of ionization of Ar in these flows, which may gain part of its energy from the hydroxyl ion [6], which has a higher ionization energy than Ar (13 eV) [23]

ISSN: 2583-4053
Volume-3 Issue-1 || February 2024 || PP. 99-108
https://doi.org/10.55544/jrasb.3.1.17

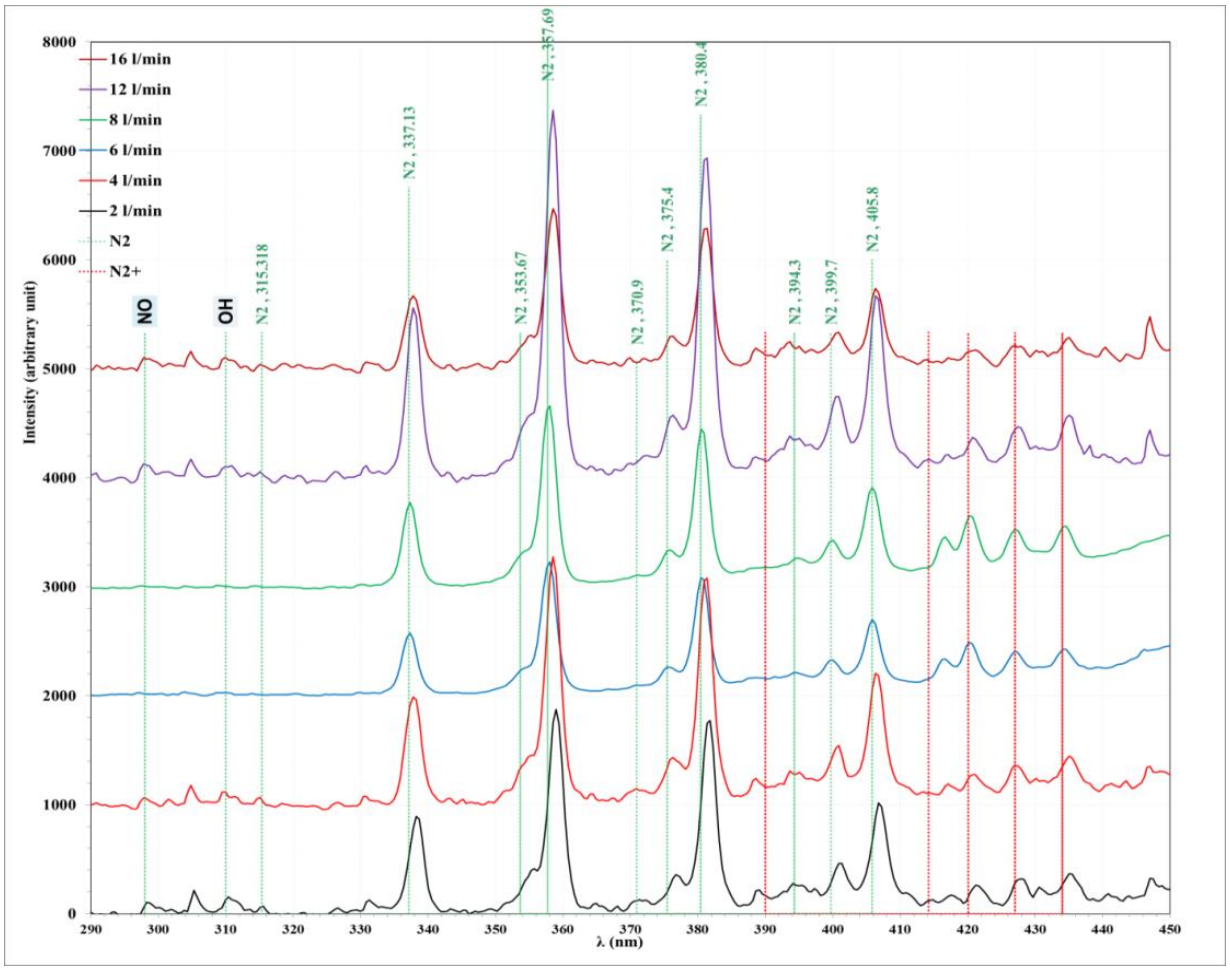

Figure 8: Molecular spectra of nitrogen emitted from plasma jet technology using different flow rates of Ar

IV. CONCLUSIONS

This study explains the impact of gas flow rate from the plasma jet system on optical emission spectroscopy outcomes. The observed trends in emission line intensity provide insights into principles leading energy distribution and collision dynamics. Notably, the maximum electron number density is achieved at an argon flow rate of 8 l/min, while the electron temperature decreases with increasing flow rate. These variations extend to other plasma parameters, illustrating the intricate interplay of plasma behavior and its interactions with external fields or electromagnetic radiations. A portion of the excitation energy of argon is transferred to nitrogen molecules, and generation of reactive species such as OH and NO, the abundance of which is contingent upon the flow rate. The most efficient flow rate is determined to be 6 l/min. The outcomes of this study hold significant promise for advancing plasma jet technology in sterilization or treatment applications.

REFERENCES

[1] J.-X. Zhang and Z.-Y. Zhao, "A comprehensive review on the preparation and applications of delafossite CuAlO2 optoelectronic functional materials," *Mater. Sci. Semicond. Process.*, vol. 167, p. 107819, 2023.
[2] X. Dai, K. Bazaka, E. Thompson, and K. (Ken) Ostrikov, "Cold Atmospheric Plasma : A Promising Controller of Cancer Cell States," *cancers Rev.*, vol. 12, p. 3360, 2020.
[3] T. Dufour, "From Basics to Frontiers: A Comprehensive Review of Plasma-Modified and Plasma-Synthesized Polymer Films," *Polymers (Basel).*, vol. 15, p. 3607, 2023.
[4] W. Van Gaens, S. Iseni, K. Weltmann, S. Reuter, and A. Bogaerts, "Numerical analysis of the effect of nitrogen and oxygen admixtures on the chemistry of an argon plasma jet operating at atmospheric pressure," *New J. Phys.*, vol. 17, p. 033003, 2015.
[5] E. H. Choi, H. S. Uhm, and N. K. Kaushik, "Plasma bioscience and its application to medicine," *Choi al. AAPPS Bull.*, vol. 31:10, pp. 1–38, 2021.
[6] C. Heslin, D. Boehm, V. Milosavljevic, and P. J. Cullen, "Quantitative Assessment of Blood Coagulation

ISSN: 2583-4053
Volume-3 Issue-1 || February 2024 || PP. 99-108
https://doi.org/10.55544/jrasb.3.1.17

by Cold Atmospheric Plasma," no. March, 2015.
[7] S. T. Hsieh, H. Mishra, N. Bolouki, W. Wu, C. Li, and J. H. Hsieh, "The Correlation of Plasma Characteristics to the Deposition Rate of Plasma Polymerized Methyl Methacrylate Thin Films in an Inductively Coupled Plasma System," *Coatings*, vol. 12, no. 7, 2022.
[8] W. Diyatmika, C.-Y. Cheng, and J.-W. Lee, "Fabrication of Cr-Si-N coatings using a hybrid high-power impulse and radio-frequency magnetron co-sputtering: The role of Si incorporation and duty cycle," *Surf. Coatings Technol.*, vol. 403, p. 126378, 2020.
[9] V. Unnikrishnan, K. Alti, V. Kartha, C. Santhosh, G. Gupta, and B. Suri, "Measurements of plasma temperature and electron density in laser-induced copper plasma by time-resolved spectroscopy of neutral atom and ion emissions," *Pramana - J. Phys.*, vol. 74, no. 6, pp. 983–993, 2010.
[10] R. J. E. Jaspers, "Plasma Spectroscopy," *Fusion Sci. Technol.*, vol. 61, no. 2T, pp. 384–393, 2012.
[11] A. Ajith, M. N. S. Swapna, H. Cabrera, and S. I. Sankararaman, "Comprehensive Analysis of Copper Plasma: A Laser-Induced Breakdown Spectroscopic Approach," *Photonics*, vol. 10, no. 2, 2023.
[12] J. W. Low, N. Nayan, M. Z. Sahdan, M. K. Ahmad, A. Y. Md Shakaff, A. Zakaria, and A. F. M. Zain, "Spectroscopic studies of magnetron sputtering plasma discharge in Cu/O2/ar mixture for copper oxide thin film fabrication," *J. Teknol.*, vol. 73, no. 1, pp. 11–15, 2015.
[13] E. Ha, C. Nagendra, K. Kaushik, Y. June, H. Jun, S. Lim, J. Sung, and C. Ihn, *Plasma bioscience for medicine, agriculture and hygiene applications*, vol. 80, no. 8. The Korean Physical Society, 2022.
[14] "NIST Atomic Spectra Database." .
[15] S. B. Bayram and M. V. Freamat, "Vibrational spectra of N2: An advanced undergraduate laboratory in atomic and molecular spectroscopy," *Am. J. Phys.*, vol. 80, no. 8, pp. 664–669, 2012.
[16] S. S. Hamed, "Spectroscopic Determination of Excitation Premixed Laminar Flame," *Egypt. J. Solids*, vol. 28, no. 2, pp. 349–357, 2005.
[17] "NIST Atomic Spectra Database (ver. 4.1.0)." .
[18] R. Wang, C. Yang, J. Hao, J. Shi, F. Yan, N. Zhang, B. Jiang, and W. Shao, "Influence of Target Current on Structure and Performance of Cu Films Deposited by Oscillating Pulse Magnetron Sputtering," *Coatings*, vol. 12, no. 3, p. 394, 2022.
[19] N. Konjević and W. L. Wiese, "Experimental Stark widths and shifts for spectral lines of neutral and ionized atoms," *J. Phys. Chem. Ref. Data*, vol. 19, no. 6, pp. 1307–1385, 1990.
[20] J. Weng, S. Kashiwakura, and K. Wagatsuma, "Effect of Plasma Gas and the Pressure on Spatially and Temporally Resolved Images of Copper Emission Lines in Laser Induced Plasma Optical Emission Spectrometry," *Anal. Sci.*, vol. 37, no. 2, pp. 367–375, 2021.
[21] E. Wagenaars, R. Brandenburg, W. J. M. Brok, M. D. Bowden, and H.-E. Wagner, "Experimental and modelling investigations of a dielectric barrier discharge in low-pressure argon," *J. Phys. D. Appl. Phys.*, vol. 39, no. 4, pp. 700–711, 2006.
[22] A. Ahmed, M. Salman, M. Alwazzan, and A. Meri, "Blushers component analysis for unbranded cosmetic brands: Elements' concentration levels and its effect on human body," *J. Adv. Res. Dyn. Control Syst.*, vol. 11, no. 5 Special Issue, pp. 412–419, 2019.
[23] N. U. Rehman, F. U. Khan, M. A. Naveed, and M. Zakaullah, "Determination of excitation temperature and vibrational temperature of the N2(C 3Πu, ν′) state in Ne-N 2 RF discharges," *Plasma Sources Sci. Technol.*, vol. 17, no. 2, 2008.